Materials Science & Engineering A 574 (2013) 186–190

Contents lists available at SciVerse ScienceDirect

Materials Science & Engineering A

journal homepage: www.elsevier.com/locate/msea

Microstructure evolution of Al–12Si–CuNiMg alloy under high temperature low cycle fatigue

Jinxiang Liu [a,*], Qing Zhang [a], Zhengxing Zuo [a], Yi Xiong [b], Fengzhang Ren [b], Alex A. Volinsky [c]

[a] School of Mechanical Engineering, Beijing Institute of Technology, Beijing 100081, China
[b] School of Materials Science and Engineering, Henan University of Science and Technology, Luoyang 471003, China
[c] Department of Mechanical Engineering, University of South Florida, Tampa, FL 33620, USA

ARTICLE INFO

Article history:
Received 12 October 2012
Received in revised form
26 February 2013
Accepted 12 March 2013
Available online 21 March 2013

Keywords:
Al–12Si–CuNiMg alloy
Microstructure evolution
Fatigue
Cyclic softening

ABSTRACT

Microstructure evolution of the Al–12Si–CuNiMg alloy under high temperature low cycle fatigue was investigated with scanning and transmission electron microscopy. The alloy exhibits cyclic softening at diverse total strain amplitudes and loading temperatures. The material fatigue life obviously decreases with the increase of the strain amplitude at the same temperature. However, fatigue life increases and microstructure improves with temperature increase at the same strain amplitude. At certain loading temperatures and strain amplitudes, the microstructure can be refined. The fracture morphology changes gradually from brittle quasi-cleavage fracture, with numerous small cracks, to quasi-cleavage fracture with numerous small dimple gliding fractures.

1. Introduction

Al–Si alloys have been widely used as piston components due to the good wear resistance, low thermal expansion coefficient, volume stability and good thermal conductivity. However, because pistons actually work under the cyclic loading, fatigue is the main form of failure. The intrinsic defects characteristics, such as the size, quantity and location of the casting defect, secondary dendrite arm spacing (SDAS), the size, quantity and shape of the eutectic Si phase, may act as crack initiation sites. These cracks expand, finally leading to the failure of the piston [1–4]. Therefore, it is important to study the fatigue behavior of cast Al–Si alloys. Numerous studies show a decrease in fatigue life with increase in the size of casting defects [5]. The larger the defect size, and the shorter the distance to the surface, the lower the fatigue life is, otherwise fatigue life is extended [6]. The SDAS is mainly determined by the cooling rate. With the decrease of the SDAS, the fracture strength and elongation of the alloy are obviously increased, and the fatigue crack initiation can be also delayed significantly [7–9]. The fatigue microcrack is easily produced near eutectic Si, so the fatigue strength is obviously increased with the size of eutectic Si phase decreasing [10,11]. However, the above reports were limited to cyclic loading at room temperature, and there is little information available on the microstructure response and fatigue behavior of cast Al–Si alloys in cyclic loading at high temperature. Due to the disadvantages of high thermal expansion coefficient, poor thermal stability and low strength at high temperature, the application of aluminum alloys as piston materials is severely limited in harsh environments. It is well known that high Si content can significantly improve the alloy flowability, decrease casting defects and increase the high temperature strength of the alloy. Meanwhile, the high temperature strength of the alloy can be improved by Cu, Ni, and Mg alloying elements, which can produce precipitate strengthening phases, such as $CuAl_2$, Mg_2Si, Al_2CuMg [12]. Therefore, the Al–12Si–CuNiMg alloy proves to be one of preferred materials for pistons in harsh environments, including high temperature, high speed, heavy loads, etc. At present, the Al–12Si–CuNiMg alloy has been comprehensively studied with regard to the high temperature tensile, thermal, creep, thermal cycling, fatigue and creep-fatigue interaction behavior [13–15]. However, the microstructure evolution of the alloy under alternate loading at high temperature is lacking of systematic and in-depth research, which seriously restricts further applications of the Al–12Si–CuNiMg alloy in automotive and aerospace industries. Therefore, the microstructure evolution of Al–12Si–CuNiMg alloy after high temperature, low cycle fatigue tests was investigated to provide experimental basis for the aluminum alloy usage in the harsh environments.

2. Materials and experimental procedures

The nominal composition of the alloy is Al–(11–13)Si–(5.0–5.5)Cu–(0.7–1.0)Mg–(2.5–3.0)Ni, in wt.%. The alloy was produced by a high pressure, squeeze casting process by BoHai Piston, Binzhou,

* Corresponding author. Tel./fax: +86 10 6891 1392.
E-mail address: liujx@bit.edu.cn (J. Liu).

0921-5093/$ - see front matter © 2013 Elsevier B.V. All rights reserved.
http://dx.doi.org/10.1016/j.msea.2013.03.027

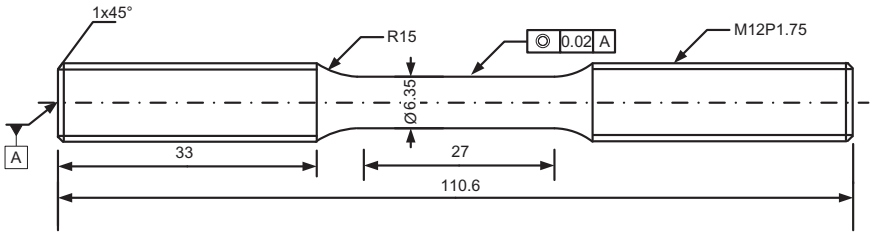

Fig. 1. Geometry of the low cycle fatigue test specimen (dimension in mm).

China. The cast material was homogenized at 750 K for 1 h, oil quenched to room temperature, retained at room temperature for 24 h. In order to obtain material properties same with the actual situation as far as possible, the analyzed alloy in the study was artificially aged at 513 K for 7.5 h. The heat treatment condition of the studied alloy are in accordance with the actual situation. The specimens used in low cycle fatigue tests have a gauge length of 27 mm and a diameter of 6.35 mm, as shown in Fig. 1.

In the study, for obtaining $\Delta\varepsilon_t$–N and $\Delta\varepsilon_p$–N curves, the cyclic stress response and microstructure evolution in the loading process, low cycle fatigue test under total strain control, which is effective and economical of cost, especially for high temperature test, was conducted. A servo-hydraulic machine (MTS-810) equipped with a heated furnace was used to perform the low cycle fatigue test at high temperatures. Before loading, the specimens were heated and kept at the test temperature for 30 min to ensure a uniform temperature throughout the specimen. The total strain, $\Delta\varepsilon$, ranging from $\pm 0.15\%$ to $\pm 0.40\%$ was applied with a constant strain rate of 3×10^{-3} s^{-1}. A symmetrical triangular waveform was used with a load ratio of $R=-1$. The real-time stress and strain data were recorded and saved to evaluate the cyclic deformation behavior of the alloy.

A JSM-5610LV (JOEL, Japan) scanning electron microscope (SEM), coupled with the compositional analysis, using an energy dispersive spectroscopy (EDS), was used to characterize both the microstructure and fracture surface. Microstructure evolution of the Al–12Si–CuNiMg alloy at different strain amplitudes and different loading temperatures was investigated by using an H-800 (Hitachi, Japan) transmission electron microscope (TEM), operated at 200 kV. TEM samples were taken from the distance of 1 mm from the fatigue fracture. Mechanically polished 40 μm thin foil was utilized for TEM sample preparation, using double jet electrolytic thinning technique (20–25 V, 50 mA) in a solution, consisting of 70 vol.% methanol + 30 vol.% HNO_3. Liquid nitrogen was used for cooling during the thinning process with the temperature not higher than −25 °C.

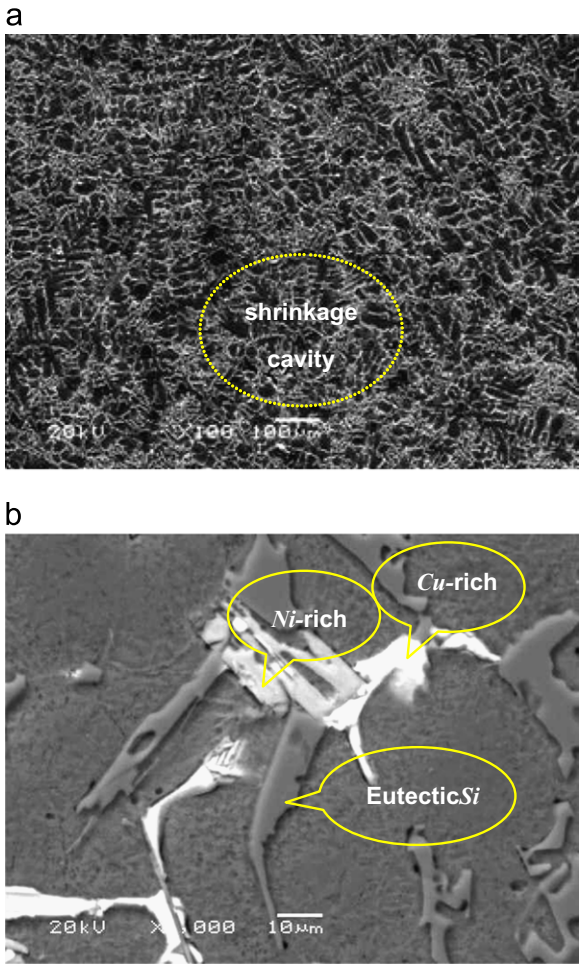

Fig. 2. (a) Original microstructure of the Al–12Si–CuNiMg alloy, (b) phases identified based on the SEM/EDS analysis.

3. Results and discussion

The original organization morphology of the Al–12Si–CuNiMg alloy is shown in Fig. 2. It clearly shows that the microstructure of the alloy primarily consists of dendritic grains, uniformly distributed large, angular silicon platelets, and fine intermetallic particles embedded in aluminum solid solution phase. Meanwhile, the shrinkage cavity defects are also present, mainly due to the lack of the feeding in the pouring process. Examination of the microstructure at higher magnifications reveals that the alloy is strengthened by large volume fractions of Cu-rich (bright white), Ni-rich (light gray) and intermetallic compounds, as seen in Fig. 2b. Evidently, Si platelets are widely distributed in the alloy. The Si platelets are intended to be disintegrated and spheroidized at high temperature during the low cycle fatigue [16]. Compared with large and elongated Si platelets, the spherical Si particles fracture less frequently [17].

Fig. 3 shows the $\Delta\varepsilon_p$–N curves of the Al–12Si–CuNiMg alloy at different loading temperatures. It can be seen that the strain amplitude has a significant effect on the fatigue life. The fatigue life of the studied material decreases with the increase of the strain amplitude at the same temperature. With the increase of the loading temperature, at any particular strain amplitude, the fatigue life of the material obviously increases.

The cyclic stress response (CSR) of the alloy was analyzed in terms of the variation of the stress amplitudes with elapsed fatigue cycles. For diverse total strain amplitudes, the alloy shows the cyclic softening effect at 200, 350 and 400 °C, as shown in Fig. 4. The studied aluminum alloy exhibits moderate cyclic softening behavior at 200 °C, as shown in Fig. 4a. At 350 and 400 °C, continuous softening can be seen and becomes stronger with increasing total strain amplitudes, as indicated in Fig. 4b and c. The cyclic softening behavior of the alloy presents a strong dependence on the total strain amplitude and temperature.

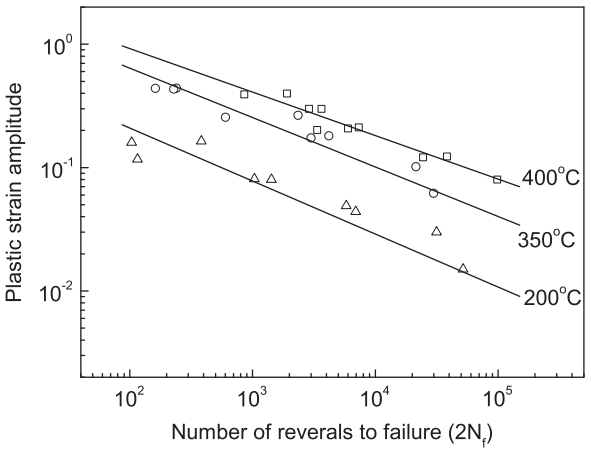

Fig. 3. Plastic strain amplitude versus number of reversals to failure at 200, 350 and 400 °C.

The cyclic softening in precipitate strengthened aluminum alloys is attributed to one or more possible mechanisms, such as ageing inhomogeneities, precipitate reversion, or resolutioning [18], over-ageing precipitate shearing and disordering [19,20], and macro-cracking. The softening in the present alloy could be due to dislocations interactions with the precipitates, which is consistent with the previous reports [21,22]. Studies are in progress to determine the exact nature of these microstructural changes at different stages of cyclic softening.

Fig. 5 shows the surface fracture morphology of the Al–12Si–CuNiMg alloy with the strain amplitude of 0.2% at 200, 350, and 400 °C, respectively. It can be seen that the fracture surface shows a quasi-cleavage fracture at 200 °C. The mixture of quasi-cleavage fracture with a high density of microcracks of the silicon platelets and other brittle constituent particles can be observed in Fig. 5a. With the temperature increasing to 350 °C, the surface fracture morphology is still brittle quasi-cleavage fracture, but a large number of tear edges can be found in Fig. 5b. Meanwhile, microcracks of the silicon platelets and the other brittle constituent particles almost disappeared. In Fig. 5c, the mixture of brittle quasi-cleavage fracture silicon platelets and ductile fracture of high density microdimples can be seen at 400 °C.

Fig. 6 shows the TEM micrographs of the fatigue failure samples of the Al–12Si–CuNiMg alloy. Fig. 6a shows the microstructure of the Al–12Si–CuNiMg alloy after aging treatment. The long strip and massive precipitated phases distributed in the Al matrix play a role in pinning dislocations and strengthening the matrix. Because the microstructure after aging didn't endure the cycle loading, the dislocations tangling around the precipitated phase can't be observed in Fig. 6a. Fig. 6b–d shows the microstructure morphology with the strain amplitude of 0.2% at 200, 350, and 400 °C, respectively. It can be seen that a large number of dislocation lines are produced in the Al matrix under the cyclic loading, and dislocation tangles and cells can be formed, as seen in Fig. 6b. Meanwhile, the shape of precipitated phase transforms from long and massive strips to globular. According to the Gibbs–Thomson effect, spheroidization of the cementite lamellae is a spontaneous process. The particle size of long strip precipitated phase is smaller than the massive precipitated phase after spheroidizing, as seen in Fig. 6b. With the temperature increase, the precipitated phase is spheroidizing at the same time, due to the Orowan's effect, and the precipitated phase is constantly coarsening. Therefore, the precipitated phase obviously reduces. As a result, the effect of dislocations pinning decreases and the dislocations mobility increases. The dislocation cell forms the subgrain boundaries, so the Al matrix is refined effectively, and the size of the

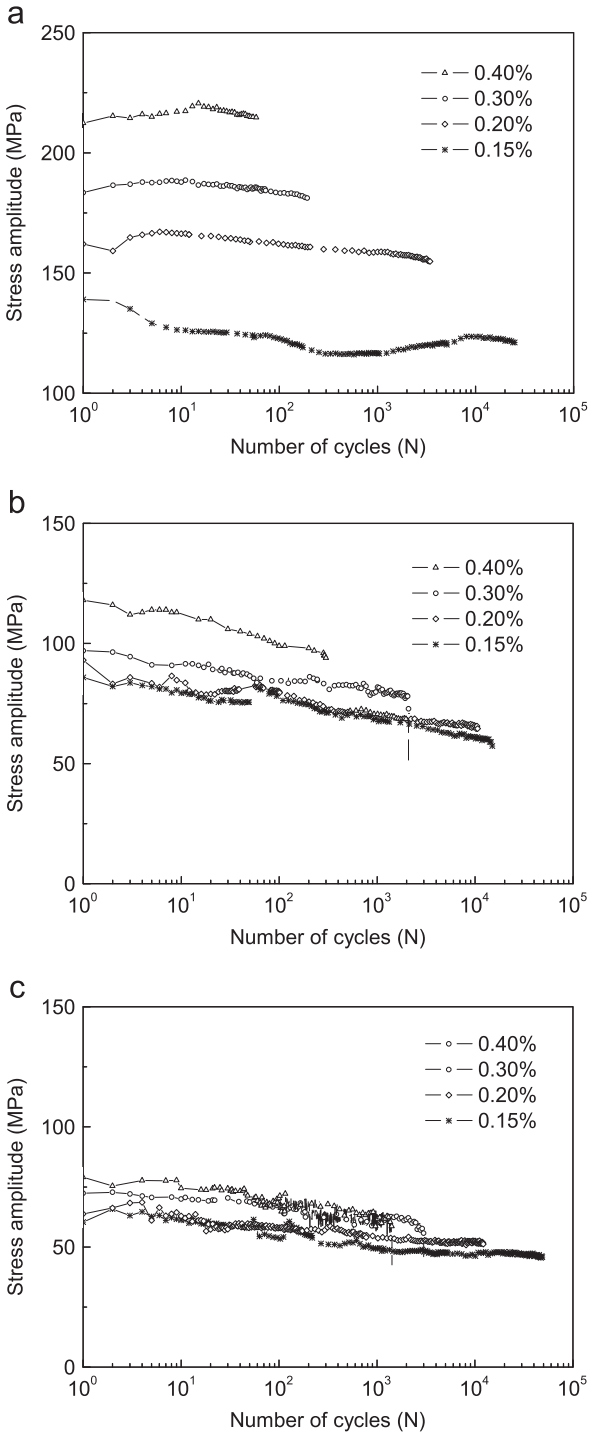

Fig. 4. Cyclic stress response at: (a) 200, (b) 350, and (c) 400 °C.

subgrain boundary is about 200 nm, as can be seen in Fig. 6c. With the temperature increasing to 400 °C, due to the dynamic recrystallization, the long strip and block precipitated phase disappear completely, replaced by numerous small precipitated phase particles with the size of about 10 nm. These precipitated phases are dispersed in the Al matrix. Meanwhile, a small amount of dislocation lines appear in the Al matrix, as seen in Fig. 6d.

Fig. 6e and f shows the microstructure morphology at 350 °C with the strain amplitude of 0.15% and 0.4%, respectively. When the strain amplitude is low, a large number of dislocation tangles can be found in the local area, at the same time, the elongated subgrain has been partly formed with the size of about 250 nm, as

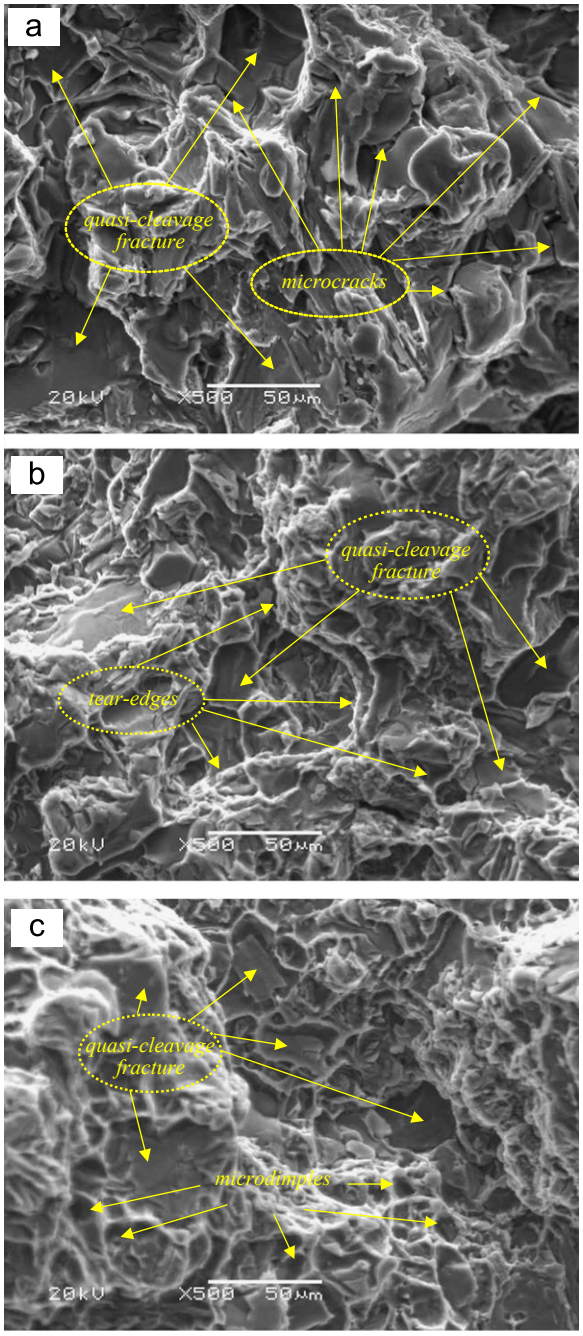

Fig. 5. Fracture surface morphology of the Al–12Si–CuNiMg alloy after 0.2% fatigue test at: (a) 200, (b) 350, and (c) 400 °C.

seen in Fig. 6e. With the increase of the strain amplitude, dislocation tangles and dislocation cells completely transform into the subgrain boundaries. Therefore, the Al matrix is refined effectively with the size of about 300 nm, as can be seen in Fig. 6f. The grain refinement mechanism can be summarized as the following process: (1) development of dislocation lines in original grains; (2) the formation of dislocation tangles and dislocation cells due to the pile-up of dislocation lines; (3) with the increase of strain amplitude, transformation of dislocation tangles and dislocation cells into subgrain boundaries; and (4) evolution of the continuous dynamic recrystallization in subgrain boundaries to refined grain boundaries.

Due to the interaction between dislocations and precipitated phase, as well as dislocations and grain or subgrain boundaries during the fatigue cyclic loading process, the dislocation movement is strongly hindered. As a result, the stress increases when the external load increased to keep constant strain, and this process can be called cyclic strain hardening. Meanwhile, the annihilation of dislocations or reconstruction of the substructure happened during the dislocation proliferation process. The dislocation density reduces, which results in the decrease of the resistance of the sliding motion. This process can be called cycle strain softening. When the rates of proliferation and annihilation are in balance, the hardening and softening effects can cancel each other out, so that the stress amplitude can remain the same during the cyclic deformation process, thus the alloy exhibits cycle stability.

In this study, the Al–12Si–CuNiMg alloy shows various phenomena of cyclic softening with different temperatures. A large number of dislocation lines are produced in the Al matrix by the strain amplitude, which shows the hardening effect. However, dynamic recovery and dynamic recrystallization are taking place in the Al matrix at elevated temperature. Dislocation annihilation and the rate of the substructure reconstruction increase significantly, leading to a softening effect. With the temperature increase, the softening effect is obviously prevailing over the hardening effect. Therefore, cyclic softening effect of the Al–12Si–CuNiMg alloy is not obvious at 200 °C, but with the increase of the temperature, the cyclic softening is obvious, and the peak stress decreases significantly. On the other hand, with the increase of cyclic loading temperature, the casting defects in the Al matrix are obviously improved. The shrinkage cavity reduces, and even disappears completely. Under the same strain amplitude, the fatigue life at high temperature is superior to that at low temperature, as seen in Fig. 4. The microcracks are effectively closed and the Al matrix is obvious refined in the cyclic loading process, as seen in Fig. 6c, e and f. The refinement of Al matrix can be attributed to the development of the dislocation and substructure. At the same time, the SDAS is decreased. All of these factors caused the increase of the fatigue resistance in the Al–12Si–CuNiMg alloy, meanwhile, the material shows high ductility.

In general, low cycle fatigue life of metals decreases with temperature under the same strain loading, whether from the standpoint of material damage, or most previously reported experimental results [23,24]. However, there have been studies reporting the similar trend as obtained in this study. In the low cycle fatigue studies of some Ni-based superalloys, the fatigue resistance, improved by high temperature, can be found in the literature [25]. Based on the analysis of cyclic deformation behavior and microstructure evolution, it is clear that, for the studied Al–12Si–CuNiMg alloy, enhanced fatigue resistance at higher temperatures is mainly attributed to the improvement of the microstructure, as well as relatively higher ductility.

4. Conclusions

The cyclic softening responses of the Al–12Si–CuNiMg alloy were observed under the diverse total strain amplitudes and cyclic loading temperatures. The fatigue life of the alloy at different strain amplitudes increases with the temperature increase. The fracture morphology changes from quasi-cleavage fracture, with numerous small cracks, to quasi-cleavage fracture with a large number of tear edges, then to quasi-cleavage fracture with numerous small dimple gliding fractures. The microstructure of the Al–12Si–CuNiMg alloy is refined under high temperature low cycle fatigue and the corresponding grain refinement mechanism is as follows: it involves the development of dislocation lines in original grains, pile-up of dislocation lines contributes to the formation of dislocation tangles and dislocation cells, the transformation of dislocation tangles and dislocation cells into subgrain

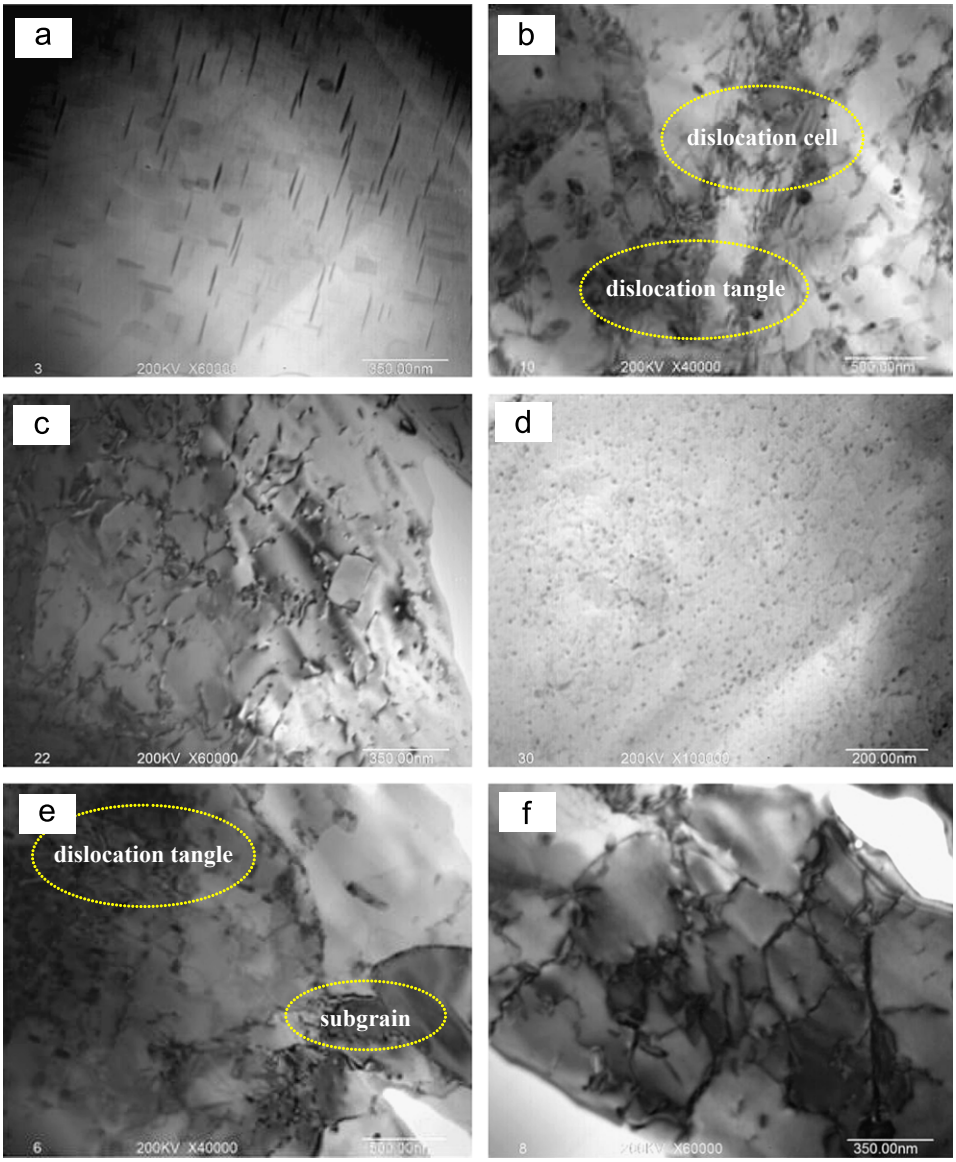

Fig. 6. TEM observation of the fatigue failure samples of the Al–12Si–CuNiMg alloy: (a) after aging, (b) 0.2% at 200 °C, (c) 0.2% at 350 °C, (d) 0.2% at 400 °C, (e) 0.15% at 350 °C, and (f) 0.4% at 350 °C.

boundaries, and the evolution of dynamic recrystallization in subgrain boundaries to refined grain boundaries.

Acknowledgments

This study is based upon work supported by the National Natural Science Foundation of China (Grant no. 51005020).

References

[1] D.A. Lados, D. Apelian, Mater. Sci. Eng. A 385 (2004) 200–211.
[2] D.A. Lados, D. Apelian, Mater. Sci. Eng. A 385 (2004) 187–196.
[3] Q.G. Wang, D. Apelian, D.A. Lados, J. Light Met. 1 (2001) 85–96.
[4] C.H. Caceres, J.R. Griffiths, Acta Mater. 44 (1996) 25–33.
[5] I.S. Batra, G.K. Dey, U.D. Kulkarni, S. Banerjee, Mater. Sci. Eng. A 359 (2003) 220–227.
[6] Q.G. Wang, D. Apelian, D.A. Lados, J. Light Met. 1 (2001) 73–74.
[7] Q.G. Wang, C.H. Caceres, Mater. Sci. Forum 242 (1997) 159–164.
[8] D.L. McDowell, Int. J. Fatigue 19 (1997) 127–135.
[9] H.R. Ammar, A.M. Samuel, F.H. Samuel, Int. J. Fatigue 30 (2008) 1024–1035.
[10] K. Gall, N. Yang, M.F. Horstemeyer, D.L. McDowell, J.H. Fan, Metall. Mater. Trans. A 30 (1999) 3079–3088.
[11] K. Gall, M.F. Horstemeyer, M.V. Schilfgaarde, M.I. Baskes, J. Mech. Phys. Solids 48 (2000) 183–2212.
[12] S. Zafar, N. Ikram, M.A. Shaikh, K.A. Shoaib, J. Mater. Sci. 25 (1990) 2595–2597.
[13] J. Bar, H.G. Klussmann, H.J. Gudladt, Scr. Metall. 29 (1993) 787–792.
[14] J. Bar, H.J. Gudladt, J. Illy, J. Lendvai, Mater. Sci. Eng. A 248 (1998) 181–186.
[15] N.E. Prasad, D. Vogt, T. Bidlingmaier, A. Wanner, E. Arzt, Mater. Sci. Eng. A 276 (2000) 283–287.
[16] S.W. Youn, C.G. Kang, Mater. Chem. Phys. 100 (2006) 117–123.
[17] A.R. Emami, S. Beguma, D.L. Chen, T. Skszek, X.P. Niu, Y. Zhang, F. Gabbianellib, Mater. Sci. Eng. A 516 (2009) 31–41.
[18] A. Abel, R.K. Ham, Acta Metall. 14 (1966) 1495–1503.
[19] C. Calabrese, C. Laird, Mater. Sci. Eng. 13 (1974) 141–157.
[20] D. Khireddine, R. Rahouadj, M. Clavel, Acta Metall. 37 (1989) 191–201.
[21] T.S. Srivatsan, Mater. Des. 23 (2002) 141–151.
[22] L.Y. Wu, Z. Yang, W.J. Xia, Z.H. Chen, L. Yang, Mater. Des. 36 (2012) 47–53.
[23] T. Ishii, K. Fukaya, Y. Nishiyama, M. Suzuki, M. Eto, J. Nucl. Mater. 258–263 (1998) 1183–1186.
[24] J. Warren, D.Y. Wei, Int. J. Fatigue 30 (2008) 1699–1707.
[25] J.J. Yu, X.F. Sun, T. Jin, N.R. Zhao, H.R. Guan, Z.Q. Hu, Mater. Sci. Eng. A 527 (2010) 2379–2389.